

International Journal of Modern Physics A
 © World Scientific Publishing Company

BOUND STATES OF THE KLEIN-GORDON EQUATION IN THE PRESENCE OF SHORT RANGE POTENTIALS

VÍCTOR M. VILLALBA* and CLARA ROJAS
Centro de Física, Apdo 21827, Caracas 1020A. Venezuela

Received (Day Month Year)
 Revised (Day Month Year)

We solve the Klein-Gordon equation in the presence of a spatially one-dimensional cusp potential. The bound state solutions are derived and the antiparticle bound state is discussed.

Keywords: Klein-Gordon equation; exact solutions; quantum effects.

1. Introduction

Since the appearance of the pioneering paper of Snyder and Weinberg¹, many articles have been published on the problem of meson fields in the presence of strong electric and gravitational fields. In 1940 Schiff, Snyder and Weinberg² carried out one of the earliest investigations of the solution of the Klein-Gordon equation with a strong external potential. They solved the problem of the square well potential and discovered that there is a critical point V_{cr} where the bound antiparticle mode appears to coalesce with the bound particle. Popov^{3,4} showed that this phenomenon is a particular effect characteristic of short range potentials and, consequently it should not be expected to be observed when one deals with Coulomb interactions^{4,5,6,7}. The asymptotic limit of the Schiff-Snyder effect, for infinite walls, has been studied by Fulling⁸. In 1979, Bawin and Lavine⁹ demonstrated that the antiparticle p -wave bound state arises for some conditions on the potential parameters, showing in this way that, for short range potentials, the presence of the Schiff-Snyder effect strongly depends on the angular momentum contribution.

The presence of strong fields introduces quantum phenomena, such as supercriticality and spontaneous pair production, that cannot be described using perturbative techniques. The discussion of overcritical behavior of bosons requires a full understanding of the single particle spectrum, and consequently of the exact solutions to the Klein-Gordon equation. Overcritical behavior associated with scalar particles in strong short range potentials could be of interest in understanding quan-

*e-mail villalba@ivic.ve

2 *Victor M. Villalba and Clara Rojas*

tum effects such as superradiance^{8,10} or particle production in the vicinity of black holes^{8,11}.

In the present article, we solve the Klein-Gordon equation for a Woods-Saxon and cusp potentials. The interest in computing bound states and spontaneous pair creation processes in such potentials lies in the fact that they possess properties that could permit us to determine how the shape of the potential affects the pair creation mechanism. We show that the antiparticle bound states arise also for the Woods-Saxon potential well, which is a smoothed out form of the square well. We also show that a cusp potential well supports antiparticle bound states.

The article is structured as follows: Sec. 2 is devoted to discuss the Klein-Gordon equation. In Sec. 3 we solve the Klein-Gordon equation in the presence of a one-dimensional Woods-Saxon potential well. We derive the equation governing the eigenvalues corresponding to the bound states and compute the bound states. In Sec. 4 we compute the bound states of the Klein-Gordon equation in the presence of an one-dimensional cusp potential well. We also show the dependence of supercritical states on the strength and shape of the potential. Finally, in Sec. 5, we briefly summarize our results.

2. The Klein-Gordon equation

The Klein-Gordon equation minimally coupled to a vector potential A^μ can be written as

$$\eta^{\mu\nu}(\partial_\mu + ieA_\mu)(\partial_\nu + ieA_\nu)\phi + m^2\phi = 0, \quad (1)$$

where the metric $\eta^{\mu\nu}$ has signature -2 , and we have set $\hbar = c = 1$. Choosing to work with a vector potential of the form,

$$eA^0 = V(\mathbf{r}), \quad \vec{A} = 0, \quad (2)$$

Eq. (1) can be written as:

$$\left(\frac{\partial}{\partial t} + iV(\mathbf{r})\right)^2 \phi - \nabla^2\phi + m^2\phi = 0. \quad (3)$$

Eq. (3) can be completely separated in spherical coordinates when one works with radial potentials^{12,13}. Analogously, we have that in Cartesian coordinates, the Klein-Gordon equation can be reduced to a second order ordinary differential equation when the potential depends only on a single space variable x . In this case Eq. (3) takes the simple form:

$$\frac{d^2\phi(x)}{dx^2} + \left[(E - V(x))^2 - m^2 - p_\perp^2\right] \phi(x) = 0, \quad (4)$$

where, since the potential $V(x)$ does not depend on time, we have separated variables in the form

$$\phi(x, t) = \phi(x) \exp(-iEt + ip_y y + ip_z z), \quad (5)$$

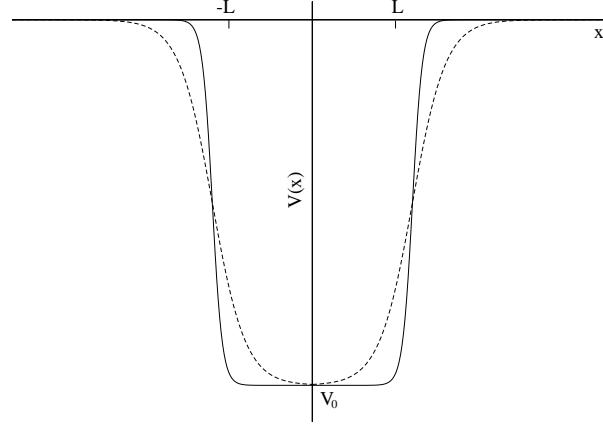


Fig. 1. The Woods-Saxon potential well for $L = 2$ with $a = 10$ (solid line) and $a = 3$ (dotted line).

and $p_{\perp}^2 = p_y^2 + p_z^2$.

Eq. (4) has the same structure than the one obtained when one solves the Klein-Gordon equation for s states, in spherical coordinates, for radial potentials^{5,12}, therefore the results reported in this article are also valid for s -waves in radial Woods-Saxon and cusp potentials. In the next section we solve Eq. (4) in the presence of a Woods-Saxon potential well.

3. The Woods-Saxon well

The Woods-Saxon potential is defined as¹⁴

$$V(x) = -V_0 \left[\frac{\Theta(-x)}{1 + e^{-a(x+L)}} + \frac{\Theta(x)}{1 + e^{a(x-L)}} \right], \quad (6)$$

where V_0 is real and positive for a well potential; $a > 0$ and $L > 0$ are real and positive. $\Theta(x)$ is the Heaviside step function. The parameter a defines the shape of the barrier or well. The form of the Woods-Saxon potential is shown in Fig. 1. In order to solve the one-dimensional Klein-Gordon equation (4), with $p_{\perp} = 0$, in the presence of the Woods-Saxon potential (6) we split the solutions into two regions. Let us consider bound states solutions for $x < 0$. In this case we need to solve the ordinary differential equation

$$\frac{d^2 \phi_L(x)}{dx^2} + \left[\left(E + \frac{V_0}{1 + e^{-a(x+L)}} \right)^2 - 1 \right] \phi_L(x) = 0, \quad (7)$$

where in Eq. (7) and thereafter we have equated the mass m to unity. Since the potential (6) depends only on one space variable, the contribution of the transverse

4 *Victor M. Villalba and Clara Rojas*

momentum in Eq. (4) appears via the introduction of an additive term that can be included in an effective mass term m_{eff} of the form $m_{eff} = (m^2 + p_{\perp}^2)^{1/2}$. For small values of p_{\perp} , the contribution of the transverse momentum does not introduce qualitative changes to the energy spectrum.

On making the substitution $y^{-1} = 1 + e^{-a(x+L)}$, Eq. (7) becomes

$$a^2 y(1-y) \frac{d}{dy} \left[y(1-y) \frac{d\phi_L(y)}{dy} \right] + \left[(E + V_0 y)^2 - 1 \right] \phi_L(y) = 0. \quad (8)$$

Setting $\phi_L(y) = y^{\sigma}(1-y)^{\gamma} h(y)$ and substituting it into Eq. (8), we obtain the hypergeometric equation

$$y(1-y)h'' + [(1+2\sigma) - 2(\sigma+\gamma+1)y]h' - \left(\frac{1}{2} + \sigma + \gamma + \lambda\right) \left(\frac{1}{2} + \sigma + \gamma - \lambda\right) h = 0, \quad (9)$$

where the prime denotes a derivative with respect to y and the parameters σ , γ , and λ are

$$\sigma = \frac{\sqrt{1-E^2}}{a}, \quad (10)$$

$$\gamma = \frac{\sqrt{1-(E+V_0)^2}}{a}, \quad \lambda = \frac{\sqrt{a^2 - 4V_0^2}}{2a}. \quad (11)$$

The general solution of Eq. (9) can be expressed in terms of Gauss hypergeometric functions¹⁵:

$$h(y) = a_1 {}_2F_1 \left(\frac{1}{2} + \gamma + \sigma - \lambda, \frac{1}{2} + \gamma + \sigma + \lambda, 1 + 2\sigma; y \right) + a_2 y^{-2\sigma} {}_2F_1 \left(\frac{1}{2} + \gamma - \sigma - \lambda, \frac{1}{2} + \gamma - \sigma + \lambda, 1 - 2\sigma; y \right), \quad (12)$$

so

$$\phi_L(y) = a_1 y^{\sigma} (1-y)^{\gamma} {}_2F_1 \left(\frac{1}{2} + \gamma + \sigma - \lambda, \frac{1}{2} + \gamma + \sigma + \lambda, 1 + 2\sigma; y \right) + a_2 y^{-\sigma} (1-y)^{\gamma} {}_2F_1 \left(\frac{1}{2} + \gamma - \sigma - \lambda, \frac{1}{2} + \gamma - \sigma + \lambda, 1 - 2\sigma; y \right). \quad (13)$$

Now we consider the solution for $x > 0$. We solve the differential equation

$$\frac{d^2 \phi_R(x)}{dx^2} + \left[\left(E + \frac{V_0}{1 + e^{a(x-L)}} \right)^2 - 1 \right] \phi_R(x) = 0. \quad (14)$$

After making the substitution $z^{-1} = 1 + e^{a(x-L)}$, Eq. (14) can be written as:

$$a^2 z(1-z) \frac{d}{dz} \left[z(1-z) \frac{d\phi_R(z)}{dz} \right] + \left[(E + V_0 z)^2 - 1 \right] \phi_R(z) = 0. \quad (15)$$

Introducing $\phi_R(z) = z^{\sigma}(1-z)^{-\gamma} g(z)$ and substituting it into Eq. (15), we obtain that $\phi_R(z)$ satisfies the hypergeometric equation:

$$z(1-z)g'' + [(1+2\sigma) - 2(\sigma-\gamma+1)z]g' - \left(\frac{1}{2} + \sigma - \gamma + \lambda\right) \left(\frac{1}{2} + \sigma - \gamma - \lambda\right) g = 0, \quad (16)$$

where the prime denotes a derivative with respect to z . The general solution of Eq. (16) is ¹⁵:

$$g(z) = b_1 {}_2F_1\left(\frac{1}{2} - \gamma + \sigma - \lambda, \frac{1}{2} - \gamma + \sigma + \lambda, 1 + 2\sigma; z\right) + b_2 z^{-2\sigma} {}_2F_1\left(\frac{1}{2} - \gamma - \sigma - \lambda, \frac{1}{2} - \gamma - \sigma + \lambda, 1 - 2\sigma; z\right), \quad (17)$$

so

$$\phi_R(z) = b_1 z^\sigma (1-z)^{-\gamma} {}_2F_1\left(\frac{1}{2} - \gamma + \sigma - \lambda, \frac{1}{2} - \gamma + \sigma + \lambda, 1 + 2\sigma; z\right) + b_2 z^{-\sigma} (1-z)^{-\gamma} {}_2F_1\left(\frac{1}{2} - \gamma - \sigma - \lambda, \frac{1}{2} - \gamma - \sigma + \lambda, 1 - 2\sigma; z\right). \quad (18)$$

As $x \rightarrow -\infty$ we have that y goes to zero, Analogously, as $x \rightarrow \infty$, z also goes to zero. We choose the regular wave functions

$$\phi_L(y) = a_1 y^\sigma (1-y)^\gamma {}_2F_1\left(\frac{1}{2} + \gamma + \sigma - \lambda, \frac{1}{2} + \gamma + \sigma + \lambda, 1 + 2\sigma; y\right). \\ \phi_R(z) = b_1 z^\sigma (1-z)^{-\gamma} {}_2F_1\left(\frac{1}{2} - \gamma + \sigma - \lambda, \frac{1}{2} - \gamma + \sigma + \lambda, 1 + 2\sigma; z\right). \quad (19)$$

In order to find the energy eigenvalues, we impose that the right and left wave functions and their first derivatives must be matched at $x = 0$. This condition leads to

$$\frac{1}{1+2\sigma} \left[\left(\frac{1}{2} + \gamma + \sigma - \lambda\right) \left(\frac{1}{2} + \gamma + \sigma + \lambda\right) \times \frac{{}_2F_1\left(\frac{3}{2} + \gamma + \sigma - \lambda, \frac{3}{2} + \gamma + \sigma + \lambda, 2 + 2\sigma, (1+e^{-aL})^{-1}\right)}{{}_2F_1\left(\frac{1}{2} + \gamma + \sigma - \lambda, \frac{1}{2} + \gamma + \sigma + \lambda, 1 + 2\sigma, (1+e^{-aL})^{-1}\right)} \right. \\ \left. + \left(\frac{1}{2} - \gamma + \sigma - \lambda\right) \left(\frac{1}{2} - \gamma + \sigma + \lambda\right) \times \frac{{}_2F_1\left(\frac{3}{2} - \gamma + \sigma - \lambda, \frac{3}{2} - \gamma + \sigma + \lambda, 2 + 2\sigma, (1+e^{-aL})^{-1}\right)}{{}_2F_1\left(\frac{1}{2} - \gamma + \sigma - \lambda, \frac{1}{2} - \gamma + \sigma + \lambda, 1 + 2\sigma, (1+e^{-aL})^{-1}\right)} \right] \\ + 2\sigma(1+e^{-aL}) = 0, \quad (20)$$

which is the eigenvalue condition for the energy E . Explicit solutions of Eq. (20), giving E in terms of V_0 , can be determined numerically. We consider the range $-1 < E < 1$ for the values of E . Some aspects of the dependence of the spectrum of bound states on the potential strength V_0 are shown in Figs. 2 and 3. At some value of V_0 , a bound antiparticle state appears, it joins with the bound particle state, they form a state with zero norm at $V_0 = V_{cr}$ and then both vanish from the spectrum.

The normalization of the wave functions in Eq. (19) is given by

$$N = 2 \int_{-\infty}^{\infty} dx [E - V(x)] \phi(x)^* \phi(x). \quad (21)$$

The norm of the Klein-Gordon equation vanishes at V_{cr} , where both possible solution $E^{(+)}$ and $E^{(-)}$ meet. Fig. 2. shows that for $2.0900 < V_0 < 2.0908$ two

6 *Victor M. Villalba and Clara Rojas*

states appear, one particle (solid line), and one antiparticle state (dashed line). In Fig. 3 the same behavior is observed for $2.3462 < V_0 < 2.3463$. Particle bound states ($E^{(+)}$) and antiparticle bound states ($E^{(-)}$) correspond to $N > 0$ and $N < 0$ respectively. For $N = 0$ both solutions meet and have the same energy. Antiparticle states appear in all the cases considered. For $L = 2$, we moved the shape parameter a from 1 to 18 and, for $L = 1$, we considered $a = 10$. Fig. 4 and Fig. 5 show the behavior of the turning point (E) versus the potential parameters a and V_0 respectively. Fig. 4 shows that as the value of a increases, the energy value, for which antiparticle states appear, increases. In Fig. 5 we observe that, as the value of V_0 increases, the energy value for which antiparticle states appear decreases. This behavior indicates that square well potentials exhibit antiparticle bound states for values of E larger than for smoothed out potentials.

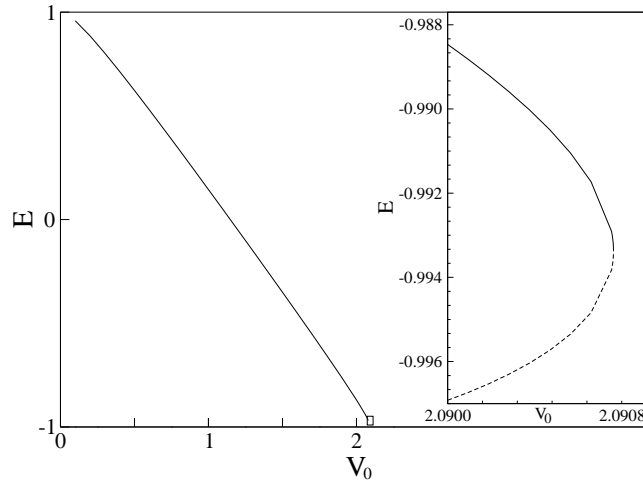


Fig. 2. Energy of the lowest bound-state spectrum for $L = 2$, $a = 10$. Inset is an enlargement of the critical area, showing solid and dotted lines corresponding to positive and negative norm state solutions respectively. The critical value for $V_0 = 2.0908$ corresponds to $E = -0.993698$. Energy is given in units of the rest energy mc^2

4. The Cusp potential well

In this section we are interested in studying the Klein-Gordon equation (4), with $p_{\perp} = 0$, in the presence of a cusp potential given by the expression ¹⁶:

$$V(x) = \begin{cases} -V_0 e^{x/a} & \text{for } x < 0, \\ -V_0 e^{-x/a} & \text{for } x > 0. \end{cases} \quad (22)$$

The form of the potential (22) is shown Fig. (6). The parameter $V_0 > 0$ determines the depth of the cusp potential well. From Fig. (6) one readily notices that the

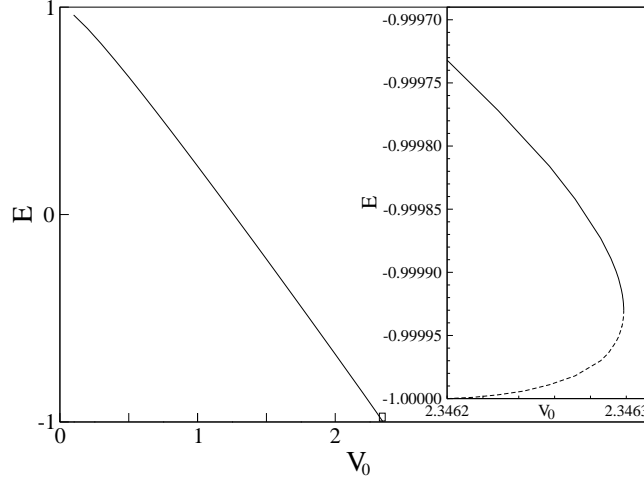


Fig. 3. Energy of the lowest bound-state spectrum for $L = 2$, $a = 2$. Inset is an enlargement of the critical area, showing solid and dotted lines corresponding to positive and negative norm state solutions respectively. The critical value for $V_0 = 2.3463$ corresponds to $E = -0.999943$. Energy is given in units of the rest energy mc^2

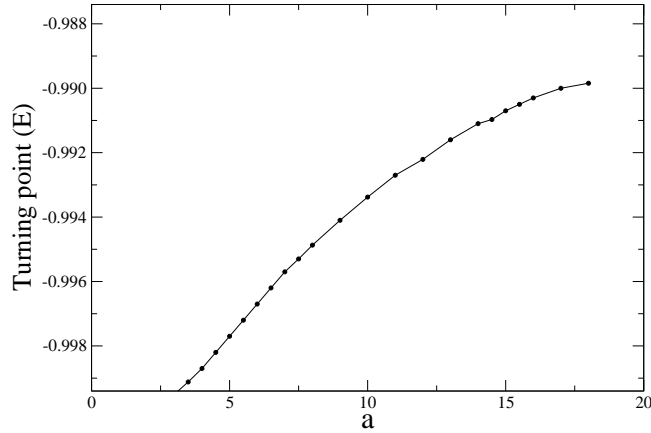


Fig. 4. Turning point versus a for $L = 2$. Energy is given in units of the rest energy mc^2

potential becomes sharper as the shape parameter a becomes smaller. In fact, the asymptotic limit of $V(x)$ as $a \rightarrow 0$ is $(-V_0/a)\delta(x)$. The potential (22) can also be regarded as a limit case of the Woods-Saxon potential well as the shape parameter $a \gg 1$ and $L = 0$ in Eq. (6). As for the Woods-Saxon potential well, we split the

8 *Victor M. Villalba and Clara Rojas*

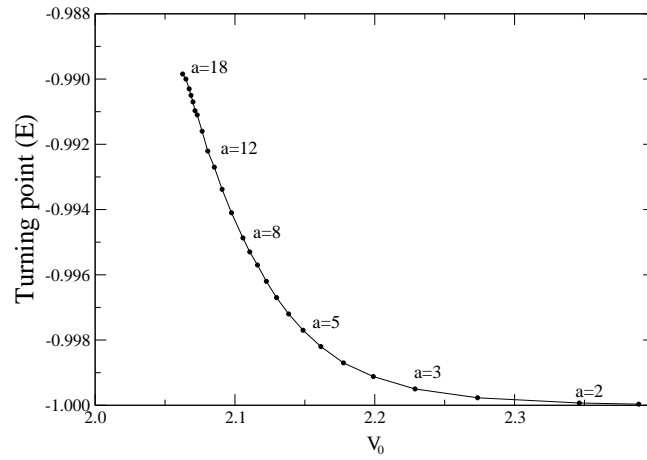


Fig. 5. Turning point versus V_0 for $L = 2$.

solutions into two regions.

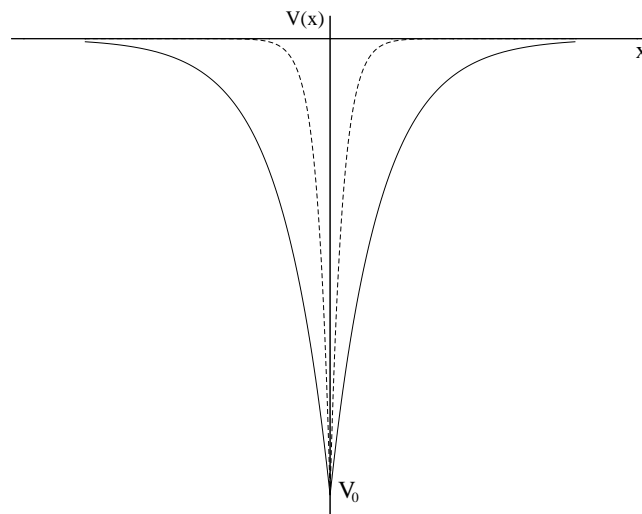


Fig. 6. The Cusp potential well for $a = 2$ (solid line) and $a = 0.5$ (dotted line).

Consider the bound states solution for $x < 0$. We solve the differential equation

$$\frac{d^2\phi_L(x)}{dx^2} + \left[\left(E + V_0 e^{x/a} \right)^2 - 1 \right] \phi_L(x) = 0. \quad (23)$$

On making the change of variables $y = 2iaV_0e^{x/a}$, Eq. (23) becomes

$$y \frac{d}{dy} \left(y \frac{d\phi_L}{dy} \right) - \left[(iaE + y/2)^2 + a^2 \right] \phi_L = 0. \quad (24)$$

Putting $\phi_L = y^{-1/2}f(y)$ we obtain the Whittaker differential equation¹⁵

$$f(y)'' + \left[-\frac{1}{4} - \frac{iaE}{y} + \frac{1/4 - a^2(1 - E^2)}{y^2} \right] f(y) = 0. \quad (25)$$

The general solution of Eq. (25) can be expressed in terms of Whittaker functions $M_{\kappa,\mu}(y)$ and $W_{\kappa,\mu}(y)$ as¹⁵

$$\phi_L(y) = c_1 y^{-1/2} M_{\kappa,\mu}(y) + c_2 y^{-1/2} W_{\kappa,\mu}(y), \quad (26)$$

where c_1 and c_2 are arbitrary constants, and κ and μ are

$$\kappa = -iaE, \quad \mu = a\sqrt{1 - E^2}. \quad (27)$$

Analogously, we proceed to obtain the solutions of Eq. (4) in the presence of the potential (22) for $x > 0$. In this case we have the differential equation

$$\frac{d^2\phi_R(x)}{dx^2} + \left[\left(E + V_0 e^{-x/a} \right)^2 - 1 \right] \phi_R(x) = 0. \quad (28)$$

On making the change of variables $z = 2iaV_0e^{-x/a}$, Eq. (28) becomes

$$z \frac{d}{dz} \left(z \frac{d\phi_R}{dz} \right) - \left[(iaE + z/2)^2 + a^2 \right] \phi_R = 0. \quad (29)$$

Putting $\phi_R = z^{-1/2}g(z)$ we obtain the differential equation

$$g(z)'' + \left[-\frac{1}{4} - \frac{iaE}{z} + \frac{1/4 - a^2(1 - E^2)}{z^2} \right] g(z) = 0, \quad (30)$$

whose general solution is

$$\phi_R(z) = d_1 z^{-1/2} M_{\kappa,\mu}(z) + d_2 z^{-1/2} W_{\kappa,\mu}(z), \quad (31)$$

where d_1 and d_2 are arbitrary constants.

Since we are looking for bound states of Eq. (4) with the potential (22), we choose to work with regular solutions $\phi_L(y)$ and $\phi_R(z)$ along the x axis:

$$\begin{aligned} \phi_L(y) &= c_1 y^{-1/2} M_{\kappa,\mu}(y), \\ \phi_R(z) &= d_1 z^{-1/2} M_{\kappa,\mu}(z). \end{aligned} \quad (32)$$

Imposing the condition that the left $\phi_L(y)$ and right $\phi_R(z)$ scalar wave functions must be continuous at $x = 0$ as well as their first derivatives, we obtain that the energy eigenvalues must satisfy the equation:

$$(1 - 2iaV_0 + 2\kappa)M_{\kappa,\mu}(2iaV_0) - (1 + 2\kappa + 2\mu)M_{\kappa+1,\mu}(2iaV_0) = 0, \quad (33)$$

The explicit solutions of Eq. (33), showing the dependence of the energy E on V_0 and a can be determined numerically. The dependence of the ground state spectrum on the potential strength V_0 is shown in Figs. (7) and (8). We can readily see that for $a = 0.5$, antiparticle states arise for $V > 3.6050$ and, for $a = 1.2$, antiparticle states arise for $V > 3.04386$. Here the solutions coming from the lower continuum into the region of bound states meet with solutions from the upper continuum. This leads to the possibility of spontaneous productions of pairs. As the Woods-Saxon potential well, with the cusp potential well, the particle bound states ($E^{(+)}$) and antiparticle bound states ($E^{(-)}$) correspond to $N > 0$ and $N < 0$ respectively. For $N = 0$ both solutions meet and have the same energy. The normalization of the wave functions (32) is given by Eq. (21). Antiparticle bound states arise for all values of the shape parameter considered. We varied the shape parameter a from 0.05 to 2.5. Figs. (9) and (10) show the behavior of the turning point (E) versus the potential parameters a and V_0 respectively. Fig. (9) shows that as the value of a increases, the energy value, for which antiparticle states appear, decreases. In Fig. (10) we observe that, as the value of V_0 increases, the energy value for which antiparticle states appear increases.

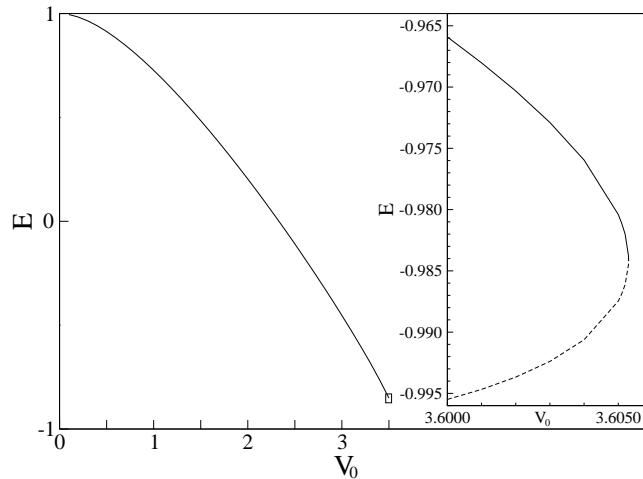


Fig. 7. Energy of the lowest bound-state spectrum for $a = 0.5$. Inset is an enlargement of the critical area, showing solid and dotted lines corresponding to positive and negative norm state solutions respectively. The critical value for $V_0 = 3.605$ corresponds to $E = -0.984766$. Energy is given in units of the rest energy mc^2

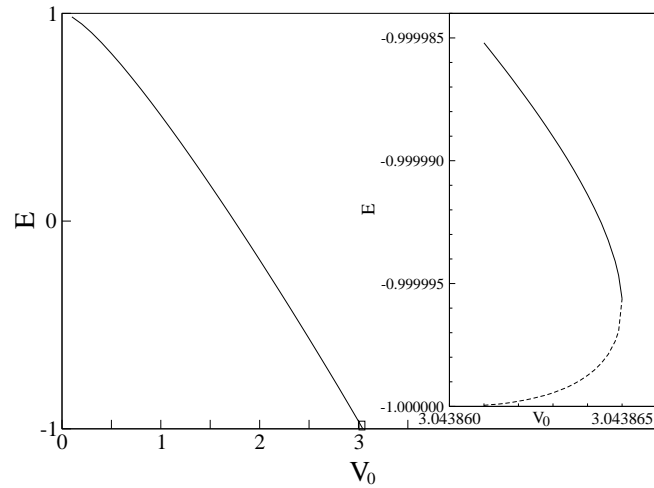


Fig. 8. Energy of the lowest bound-state spectrum for $a = 1.2$. Inset is an enlargement of the critical area, showing solid and dotted lines corresponding to positive and negative norm state solutions respectively. The critical value for $V_0 = 3.043865$ corresponds to $E = -0.999996$. Energy is given in units of the rest energy mc^2

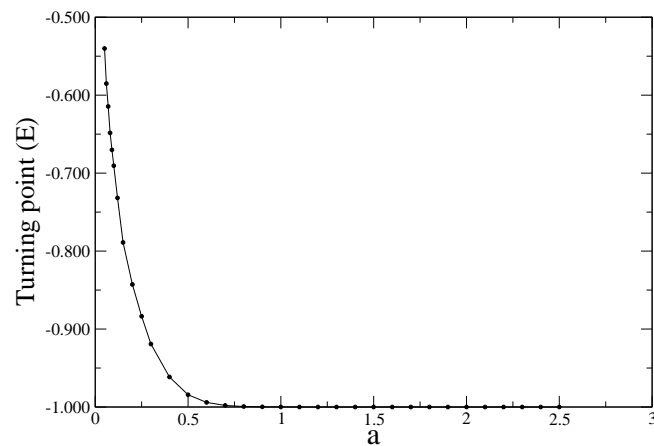


Fig. 9. Turning point versus a . Energy is given in units of the rest energy mc^2

5. Conclusions

In this article we have shown that the Woods-Saxon and the cusp potential well are able to bind scalar particles.

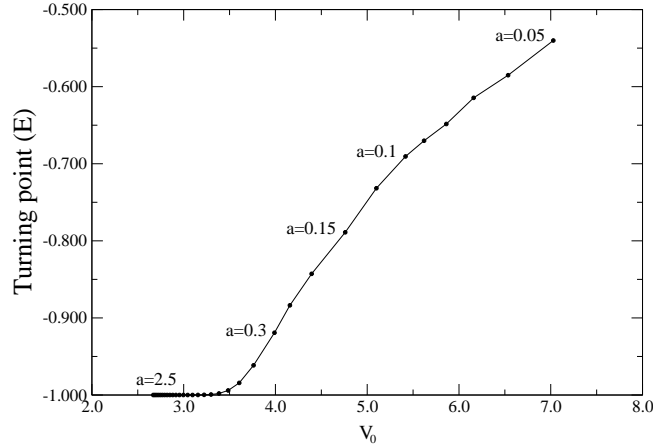


Fig. 10. Turning point versus V_0 . Energy is given in units of the rest energy mc^2

The Woods-Saxon potential, analogous to the square well potential, shows antiparticle bound states. The turning point, where the norm is zero, depends on the potential parameters a and V_0 . Therefore the one-dimensional Woods-Saxon potential exhibits a behavior characteristic of short range potentials³. It should be expected that, like in the Coulomb problem, for slow damping potentials no antiparticle bound states appear. The results reported in this article suggest that the one-dimensional Schiff-Snyder-Weinberg effect² can be extended to the case of potentials with non compact support, provided they exhibit, for large values of the space parameter, a fast damping asymptotic behavior.

Acknowledgments

This work was supported by FONACIT under project G-2001000712.

References

1. H. Snyder and J. Weinberg, *Phys. Rev.* **57**, 307 (1940).
2. L. I. Schiff, H. Snyder, J. Weinberg, *Phys. Rev.* **57**, 315 (1940).
3. V. S. Provo, *Sov. Phys. JETP* **32**, 526 (1971).
4. J. Rafelski, L. Fulcher, and A. Klein, *Phys. Rep.* **38**, 227 (1978).
5. M. Bawin and J. P. Lavine, *Phys. Rev. D* **12**, 1192 (1975).
6. A. Klein and J. Rafelski, *Phys. Rev. D.* **11**, 300 (1975).
7. A. Klein and J. Rafelski. *Phys. Rev. D.* **12** 1194 (1975).
8. S. A. Fulling, *Aspects of Quantum Field Theory in Curved Space-Time* (Cambridge, 1991).
9. M. Bawin and J. P. Lavine *Lett. Nuovo Cimento* **26**, 586 (1979).
10. Ya. B. Zel'dovich, *Sov. Phys. JETP Lett* **14**, 180 (1971).

11. N. D. Birrell and P. C. W. Davies, *Quantum Fields in Curved Space*, (Cambridge University Press, 1984).
12. W. Greiner, *Relativistic Quantum Mechanics. Wave equations*, (Springer, 1987).
13. W. Greiner, B. Müller, and J. Rafelski, *Quantum Electrodynamics of Strong Fields*, (Springer, 1985).
14. P. Kennedy, *J. Phys. A* **35**, 689 (2002).
15. M. Abramowitz and I. A. Stegun, *Handbook of Mathematical Functions*, (Dover, 1965).
16. V. M. Villalba, W. Greiner, *Phys. Rev. D* **67**, 052707 (2003).